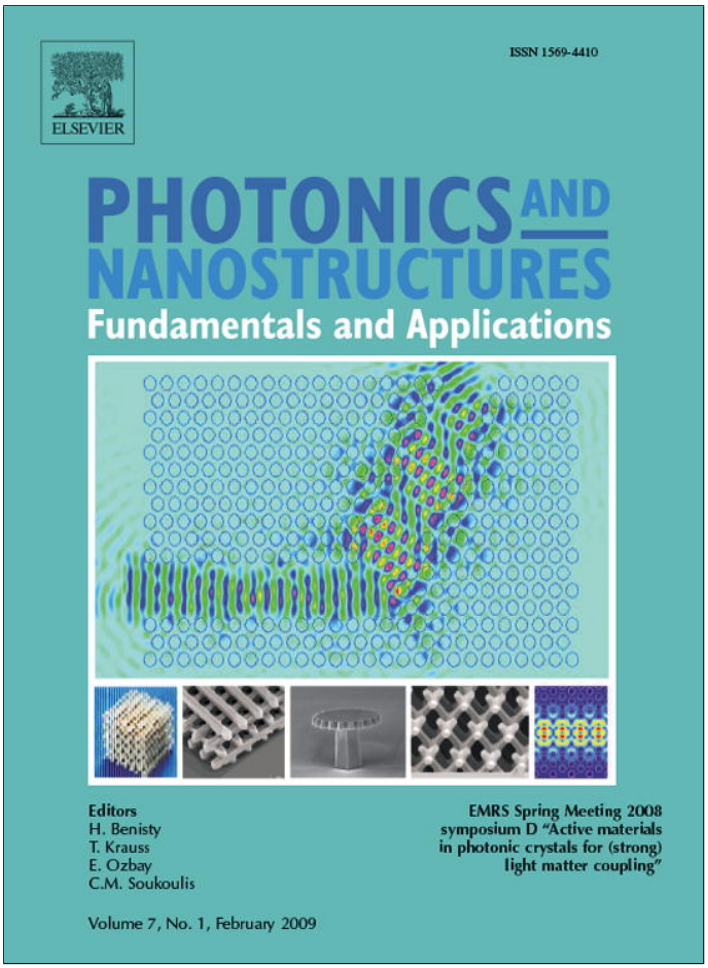

Available online at www.sciencedirect.com
ScienceDirect
Photonics and Nanostructures – Fundamentals and Applications 7 (2009) 56–62
PHOTONICS AND NANOSTRUCTURES Fundamentals and Applications
www.elsevier.com/locate/photonics

# Quantum dots in photonic crystals: From quantum information processing to single photon nonlinear optics

Dirk Englund *,[1], Ilya Fushman [1], Andrei Faraon [1], Jelena Vučković

*Ginzton Laboratory, Stanford University, 316 Via Pueblo Mall, Stanford, CA 94305, United States*

Received 4 July 2008; received in revised form 18 October 2008; accepted 19 November 2008
Available online 6 December 2008

**Abstract**

Quantum dots in photonic crystals are interesting both as a testbed for fundamental cavity quantum electrodynamics (QED) experiments and as a platform for quantum and classical information processing. We describe a technique to coherently access the QD-cavity system by resonant light scattering. Among other things, the coherent access enables a giant optical nonlinearity associated with the saturation of a single quantum dot strongly coupled to a photonic crystal cavity. We explore this nonlinearity to implement controlled phase and amplitude modulation between two modes of light at the single photon level—a nonlinearity observed so far only in atomic physics systems. We also measured the photon statistics of the reflected beam at various detunings with the QD/cavity system. These measurements reveal effects such as photon blockade and photon-induced tunneling, for the first time in solid state. These demonstrations lie at the core of a number of proposals for quantum information processing, and could also be employed to build novel devices, such as optical switches controlled at the single photon level.


*PACS :* 42.50.Ct; 42.50.Dv; 42.70.Qs; 78.67.Hc

*Keywords:* Quantum information; Single photon source; Coherent control; Giant optical nonlinearity; Photonic crystal; Quantum dot

Several proposals for scalable quantum information networks and quantum computation rely on direct probing of the cavity-quantum dot coupling by means of resonant light scattering from strongly or weakly coupled dots [1–6]. Such experiments were performed in atomic systems [7–9] and superconducting circuit QED systems [10]. In 2007, we showed that the coupling between a QD and a cavity can also be probed in solid-state systems. The quantum dot (QD) strongly modifies the cavity transmission and reflection spectra as predicted [5] (this result was simultaneously reported by Srinivasan and Painter for a QD strongly coupled to a microdisk resonator [11]). When the QD is coupled to the cavity, a weak laser beam that is resonant with its transition is prohibited from coupling to the cavity. As the average probe photon number approaches unity inside the cavity, we observe a giant optical nonlinearity as the QD saturates. This technique, which we call Coherent Optical Dipole Access in a Cavity (CODAC), represents a first major step toward quantum devices based on coherent light scattering and large optical nonlinearities from QDs in photonic crystal cavities.

## 1. Coherent access of quantum dot–cavity system

We use an L3 photonic crystal cavity [13] resonant at wavelength $\lambda_{cav} \sim 926$ nm and having quality factor

* Corresponding author. Tel.: +1 650 450 3829; fax: +1 509 277 4924
*E-mail address:* englund@stanford.edu (D. Englund).
[1] These authors contributed equally.

1569-4410/$ – see front matter © 2008 Elsevier B.V. All rights reserved.
doi:10.1016/j.photonics.2008.11.008

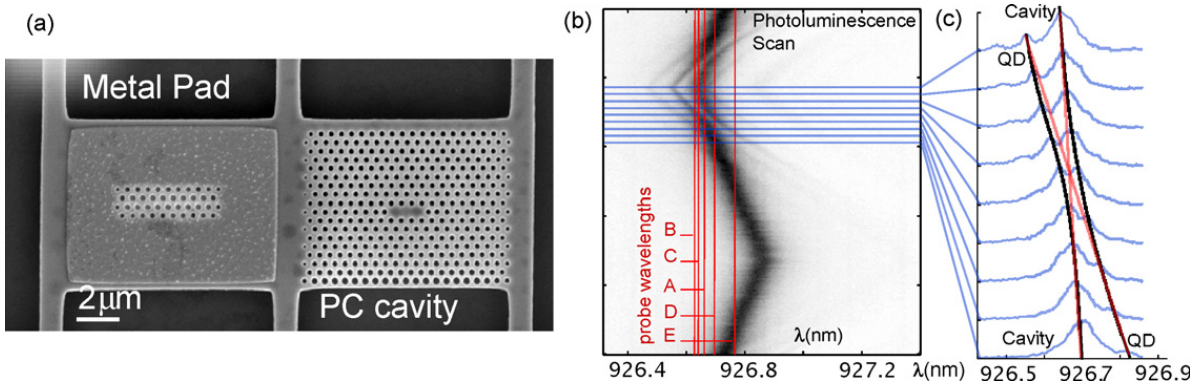


Fig. 1. (a) Photonic crystal structure containing cavity and laser heating pad. (b) The spectrum of strongly coupled QD/cavity system tuned through resonance by tuning the temperature [12]. (c) Cavity/QD anti-crossing. The red lines show the QD/cavity tuning if the two were uncoupled.

$Q = 1.0 \times 10^4$ and field decay rate $\kappa/2\pi = 16$ GHz. The structure, shown in Fig. 1(a), also contains a metal pad which is used to heat the photonic crystal with an additional laser beam [12]. The cavity is strongly coupled to a QD, with a polariton splitting of 0.05 nm. The corresponding cavity–dot coupling rate $g/2\pi = 8$ GHz. This splitting is seen in the (incoherent) photoluminescence (PL) measurements in Fig. 1(b, c), where the QD is tuned through the cavity by changing the structure's temperature. Then we probed the system coherently, by reflecting a near-resonant laser beam from the cavity. The setup and measurements are given in Ref. [14]. Briefly, the signal reflected by the cavity is monitored in cross-polarization with respect to the input beam to reduce background [15]. Then reflectivity is measured by temperature-tuning the cavity/QD resonances through the reflected narrow-linewidth probe laser beam. The probe's incident power is in the weak excitation limit corresponding to fewer than one photon inside the cavity per cavity lifetime (3 nW measured before the objective lens), as required for probing the Vacuum Rabi splitting. As the single QD sweeps across the cavity, it coherently scatters the probe laser to interfere with the cavity signal. Instead of observing a Lorentzian-shaped cavity spectrum, a drop in the reflected signal is observed at the QD wavelength with a linewidth of $g^2/\kappa$, as expected [5].

Earlier probing of the strongly coupled cavity/quantum dot system was done by photoluminescence [12,16–19]. Since excitons spontaneously recombine to produce the signal in these measurements, that technique represents an incoherent probing of the system. By contrast, the CODAC method described here represents a direct, coherent optical pathway to probe the system. The coherence results in the reflectivity dip: the quantum dot scatters photons $\pi$ out of phase with the cavity field, which results in this case in a destructive interference.

We find good agreement between the measured reflectivity and theory [14], using the above-mentioned cavity/QD parameters and the tracked QD and cavity wavelengths shown in the bottom of Fig. 2(a). The QD-

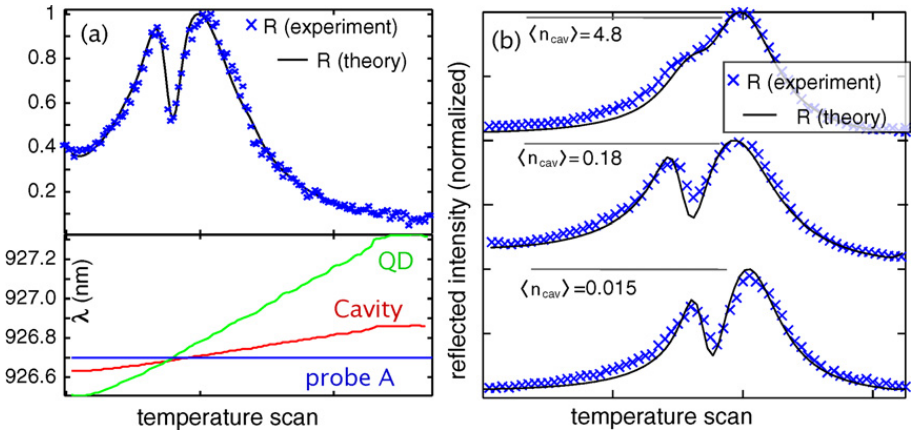


Fig. 2. Resonant probing of QD/cavity system. (a) The cavity and quantum dot are scanned across the fixed probe by temperature tuning. The reflected intensity drops when the QD becomes resonant with the probe beam. (b) The QD is saturated at extremely low power, representing a large optical nonlinearity. $\langle n_{\mathrm{cav}} \rangle$ denotes the average photon number in the cavity.

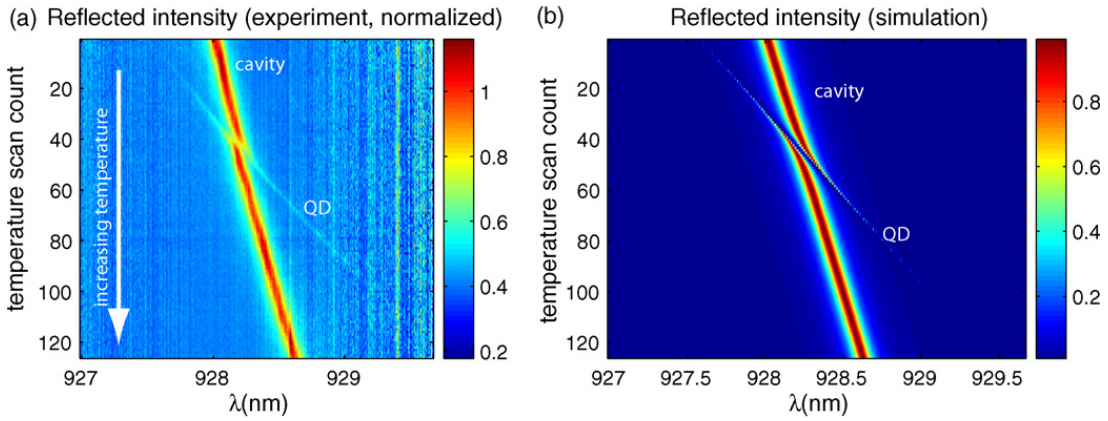


Fig. 3. (a) Broad-band cavity reflectivity from cavity, as the quantum dot is tuned through the anti-crossing point. (b) Reflected signal (theory).

induced feature does not reach zero because of fluctuations in the heating power (and hence QD resonance). When this noise is taken into account in our fit by convolving the spectrum with a Gaussian filter (FWHM = 0.005 nm), the theoretical model matches the data (black fits). Another reason why the dip does not reach closer to zero, as predicted by theory, is that the dot randomly jumps between different states which can be resonant or off-resonant from the cavity. The resonant state produces a dip while the off-resonant state does not. As a consequence, the dip height is averaged between the occupation probabilities. This 'blinking' was less significant than thermal jitter in this QD/cavity, but we have observed that it can play a big role in other systems. The reason for blinking is probably primarily random charging [20].

So far, we have shown reflectivity spectra obtained at the narrow wavelength range of the probe laser. This technique provides higher resolution than the spectrometer. However, if the quantum/cavity coupling is high, then the QD-induced feature can also be resolved when the cavity is probed with a broad-band source which is then analyzed on a spectrometer. For lack of a broad-band continuous-wave source near 928 nm, we used the Ti:Sapph laser in pulsed mode ($\sim$3 ps duration and $\sim$0.3 nm width). The probe intensity was very low, about 1 nW before the microscope's objective lens, so that the pulses do not saturate the quantum dot. The reflected signal is shown in Fig. 3(a), normalized by the roughly Gaussian spectrum of the probe. This QD/cavity system is identical in design to the one discussed above, with a $Q$ value near 10,000. The quantum dot has slightly higher coupling with $g/2\pi = 16$ GHz. Because of the limited resolution the spectrometer (0.03 nm), the features are blurred. Otherwise the reflected spectrum agrees with theory, which is plotted in Fig. 3(b). It is possible to probe the system in broad-band when its response is linear, as in this weak-excitation limit where the average intracavity photon number $\langle n\rangle \ll 1$. When the probe intensity grows, the two-level nature of the quantum dot causes a large nonlinearity. We discuss this next.

## 2. Giant optical nonlinearity

In Fig. 2(b), we show that the reflectivity of the cavity changes as the probe beam reaches $\sim$ 1 intracavity photon. $P_{\rm in}$ is increased from the low-excitation limit at 5 nW before the objective (corresponding to average cavity photon number $\langle n_{\rm cav}\rangle \approx 0.003$ in a cavity without QD) to the high-excitation regime with $P_{\rm in} \approx 12$ μW (corresponding $\langle n_{\rm cav}\rangle \approx 7.3$). Here, $\langle n_{\rm cav}\rangle$ is estimated as $\eta P_{\rm in}/2\kappa\hbar\omega_c$, where $\eta \approx 1.8\%$ is the coupling efficiency into the cavity at this wavelength. We modeled the saturation behavior by a steady-state solution of the quantum master equation following Ref. [21] using independently measured system parameters [14]. We see very good agreement over three orders of magnitude of the pump power [14].

### 2.1. Amplitude and phase control

Since the QD-induced feature is an interference between the cavity field and the dot-scattered field, we can use its rapid saturation to change the phase of a signal beam with the field of a control beam. Such a controlled phase shift is attractive for constructing two-qubit quantum logic gates with photons [22]. A controlled phase gate, which may be realized by an atom in a high quality ($Q$) cavity [23], performs this function. In this gate, the accumulated phase of one beam is conditioned on the total number of photons interacting with the atom, and the presence of other photons can be measured without destroying them

[24,9]. Based on the giant optical nonlinearity, we review in this section a conditional phase measurement [25]. We employ the same type of cavity design as described above, with a $Q$ value near 10,000. A quantum dot is strongly coupled with vacuum Rabi frequency $g/2\pi = 16$ GHz.

We measure the phase of cavity-reflected photons by interfering them with a reference beam of known intensity and phase. The setup is detailed in Ref. [25]. Briefly, the setup consists of a polarized laser beam that passes a quarter wave-plate (QWP) at an angle $\theta$ to the beam's polarization, and then reflects from the cavity and passes back through the wave plate. The component that is along the linearly polarized cavity is reflected with reflectivity $r(\omega)$, while the orthogonally polarized component reflects from the cavity and an underlying Distributed Bragg Reflector with unity reflectivity. In passing back through the QWP, these two reflected components are in general mixed. After they pass through a polarizing beam splitter (PBS), they are collected through a spectrometer on a silicon CCD. The intensity on the detector thus corresponds to interference between the reference beam, directly reflected from the sample, and the probe beam that is reflected from the cavity. The interference allows extraction of the phase difference between the reference and probe beams. Specifically, the detected signal $I_s$ is

$$I_s(\omega,\theta) = |A(\theta)(r(\omega) + e^{i\Psi(\theta)})|^2, \tag{1}$$

where $A(\theta)$ is a coefficient that depends on the QWP angle $\theta$ relative to the vertical polarization of the PBS,

$$r(\omega) = \frac{2\kappa\sqrt{\eta}}{i(\omega_c - \omega) + \kappa + (g^2/(i(\omega_d - \omega) + \gamma))} - 1, \tag{2}$$

is cavity reflectivity for a probe at frequency $\omega$, a cavity at $\omega_c$, and a QD at $\omega_d$ and having natural decay rate $\gamma/2\pi \approx 0.1$ GHz in the bulk semiconductor. $\sqrt{\eta}$ is the coupling efficiency of the probe beam (assumed to be polarized with the cavity) into and out of the cavity. $\Psi(\theta)$ is the reference phase delay:

$$e^{i\Psi(\theta)} = \frac{\cos^2(2\theta) + i\sin(2\theta)}{\cos^2(2\theta) - i\sin(2\theta)}, \tag{3}$$

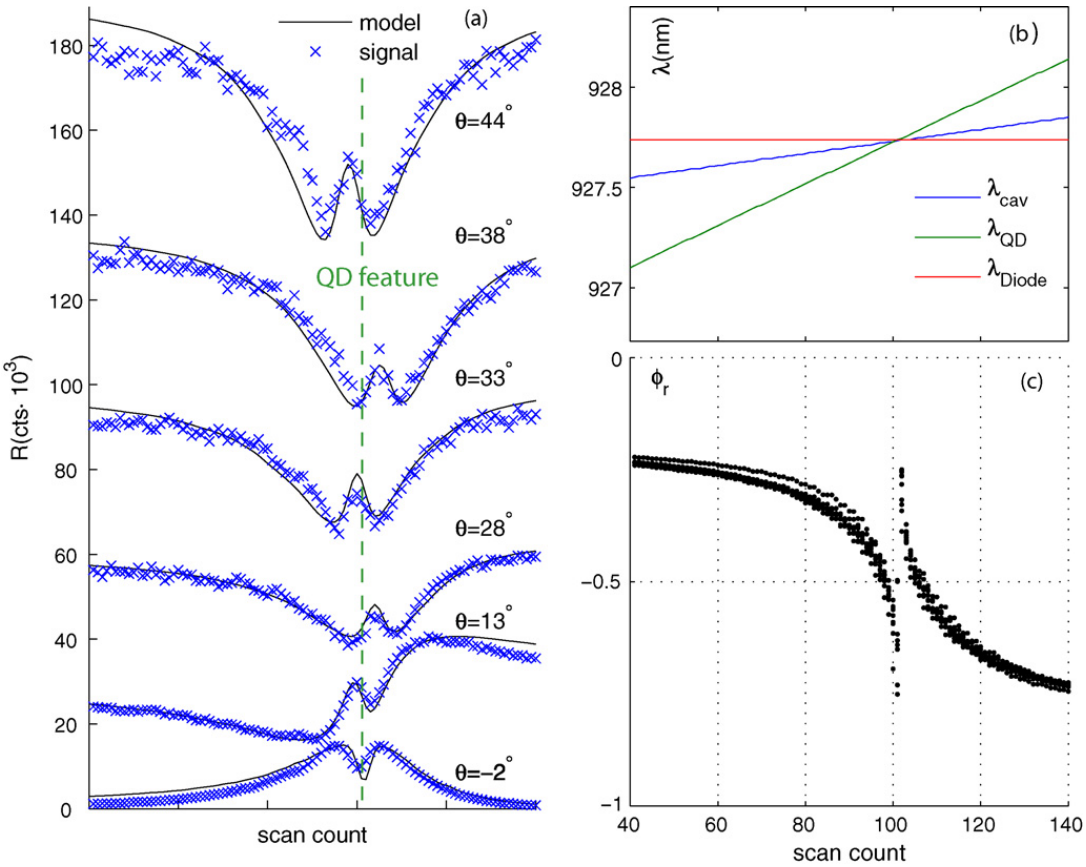


Fig. 4. (a) Measured reflectivities at different QWP settings $\theta$ as the dot and cavity are tuned through the probe beam by changing temperature (scan count). The data are fit by the model of Eq. (1). (b) Quantum dot, cavity, and probe wavelengths as a function of temperature scan. (c) Reflected phase, extracted from model Eq. (1).

The amplitude at the detector is proportional to the modulus squared of $A(\theta)$, where

$$A(\theta) = \frac{i}{2}(\cos^2(2\theta) - i\sin(2\theta)), \tag{4}$$

By changing the QWP angle $\theta$, we can produce different interference conditions between the complex cavity reflectivity $r(\omega)$ and the known $\theta$-dependent term $e^{i\Psi(\theta)}$.

### 2.1.1. Phase measurement

We deduce the phase of $r$ by fitting the observed $I_s(\omega)$ with the model of Eq. (1), as detailed in Ref. [25]. Then we can verify that the QD-induced feature is produced by an interference effect by varying the phase through $\theta$. Fig. 4(a) shows that as the phase is changed, the QD-feature evolves from destructive to constructive, and the dip at $\theta = 0°$ changes to a peak at $\theta = 33°$. Each fit to the model matches the observation well and gives the signal phase $\phi_r = \arctan(\Im m[r(\omega)]/\Re e[r(\omega)])$, where $\Re e[r(\omega)]$ and $\Im m[r(\omega)]$ are the real and imaginary parts of the cavity reflectivity $r(\omega)$. The phase fits for eleven scans with different QWP angles $\theta$ are superposed in Fig. 4(c). As the signal wavelength traverses the cavity resonance, $\phi_r$ changes from 0 to $-\pi$. An additional phase change occurs at the quantum dot resonance, where the phase varies by almost $\pi$ over the dot bandwidth ($2g^2/\kappa = 2\pi \times 32$ GHz). Instead of fitting the data by the analytical model, we can also directly deduce the real and imaginary components of the cavity reflectivity by measurements of Eq. (1) at different phases. This phase measurement is detailed in Ref. [26].

### 2.1.2. Phase control at single wavelength

When the control and signal are at nearly the same wavelength, the nonlinear interaction between them (Fig. 5(a)) arises from the saturation of the QD in the presence of cavity coupled photons [14]. We observe a phase change of $0.24\pi$ (43°) when the control photon number is increased from $n_c = 0.08$ to 3. $R/R_0$ increases from 0.5 to 1.0 at saturation. In these measurements, the wavelength is red-detuned by $\sim$0.014 nm ($g/3.5$) from the anti-crossing point (see Ref. [25]).

It may be easier to separate control and signal beams in wavelength. In that case, the signal and control beams would clearly no longer be interchangeable. But detuned beams would be suited for applications such as quantum nondemolition (QND) detection, where the control beam accumulates a phase in the presence of the signal beam, or all-optical control, where a control beam switches the transmission of the cavity to the signal beam. For this measurement, we consider another dot that is also strongly coupled with a vacuum Rabi frequency $g/2\pi = 8$ GHz. We detuned the control beam by $\Delta\lambda = -0.027$ nm ($\simeq$ g) from the signal beam. With a constant signal intracavity number $n_s \approx 0.2$, we then varied the control photon number $n_c$. The photon–photon interaction is mediated primarily by the QD saturation through the control beam, though some detuning occurs by the AC Stark effect, which can create large phase shifts [27]. In Fig. 5(b), we plot the phase and intensity of the signal beam when it is red-detuning by 0.4 g from the cavity, which in turn is resonant with the QD. Here the phase is plotted with respect to the phase when the control beam is off, $\Delta\phi_r = \phi_r - \phi_r(n_c = 0) \equiv \phi_r - \phi_{r,0}$.

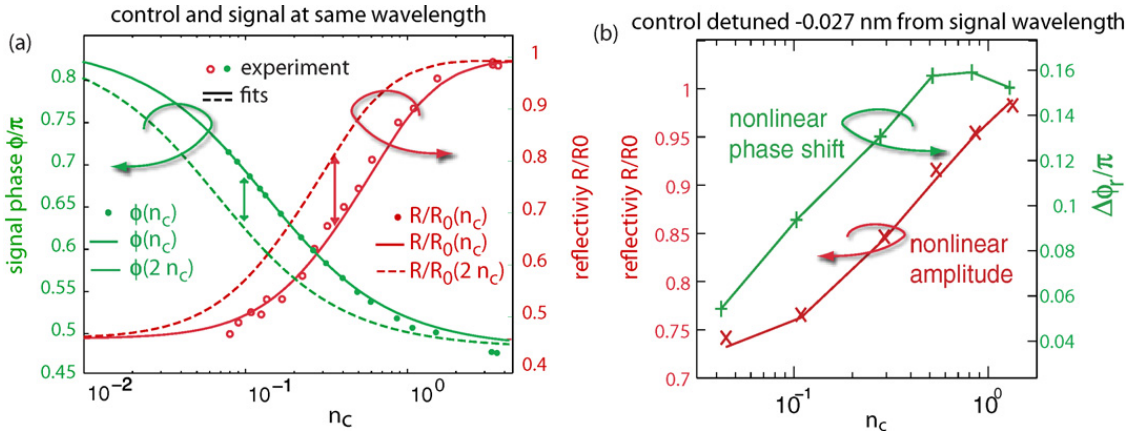


Fig. 5. Saturation of the QD-induced interference and its corresponding phase. (a) The dot was detuned from the cavity by $g/3.5$; the control and probe beams are identical here. The measured saturation agrees with theory (solid line). The dashed curves show the expected phase and intensity when the control intensity is doubled. The nonlinear phase shift $\phi_r(n_c) - \phi_r(2n_c)$ is maximized at $n_c = 0.1$, indicated by the arrow. (b) Nonlinear response to control photon number $n_c$ when the signal beam is 0.009 nm ($\approx g/3$) from the dot resonance (vertical lines in a and b).

Quantum gates require a large phase change of a signal photon, conditioned on a single control photon [23,28,29]. Furthermore, they require that both signal and control photons have the same wavelength and duration. We measured the differential phase change by the difference between the phase evaluated at $n_c$ and $2n_c$ (Fig. 5(a)). This gave a maximum differential phase shift of $0.07\pi$ (12°) at $n_c = 0.1$ and maximum amplitude change of 15% at $n_c = 0.43$. Theoretically we estimate a maximum of $\simeq 0.15\pi$ (27°) for phase and 20% amplitude modulation with our system parameters, when the quantum dot is tuned on resonance with the cavity.

A controlled phase gate requires a $\pi$ phase shift [23,30]. Relying on the saturation of the dot, this would require repeated interactions, possibly by cascading several QD/cavity systems in series. In this case, the coupling losses would grow exponentially. A more efficient, on-chip integrated architecture [31], promises to improve efficiencies. A second, though smaller, source of coherence loss is QD spontaneous emission. It is useful in this respect that the spontaneous emission into non-cavity modes is suppressed by the PC bandgap [32].

## 3. Conclusions

In conclusion, we have demonstrated a technique to coherently access a QD in a photonic crystal cavity. This photonic access enables a giant nonlinear optical response of the QD/cavity system, occurring at the single photon level [14]. This nonlinearity allows conditional phase and amplitude changes of a signal photon via a control beam [25]. Alternatively, the signal photon's phase may be changed by as much as $\pi$ by AC-stark shift of a control photon. A controlled $\pi-$ gate would enable a full set of quantum logic gates [30]. From measurements of the second-order coherence function, we also demonstrated that the cavity/QD system provides a photon–photon interaction which results in either photon blockade or photon-induced tunneling [33]. These results suggest that the QD/cavity system is very promising for quantum and classical information processing. Currently, the coupling efficiencies into and out of the cavity are still low—on the order of 2–5%. By adopting an on-chip approach and exploring better off-chip couplers, we hope to bring this efficiency near unity and thus enable efficient, controlled interactions between single photons.

## References


[1] J.I. Cirac, P. Zoller, H.J. Kimble, H. Mabuchi, Quantum state transfer and entanglement distribution among distant nodes in a quantum network, Phys. Rev. Lett. 78 (16) (1997) 3221–3224.

[2] A. Imamoğlu, D.D. Awschalom, G. Burkard, D.P. DiVincenzo, D. Loss, M. Sherwin, A. Small, Quantum information processing using quantum dot spins and cavity QED, Phys. Rev. Lett. 83 (20) (1999) 4204–4207.

[3] L.-M. Duan, H.J. Kimble, Scalable photonic quantum computation through cavity-assisted interactions, Phys. Rev. Lett. 92 (12) (2004) 127902.

[4] L. Childress, J.M. Taylor, A.S. Sorensen, M.D. Lukin, Fault-tolerant quantum repeaters with minimal physical resources and implementations based on single-photon emitters, Phys. Rev. A 72 (2005) 052330.

[5] E. Waks, J. Vučković, Dipole induced transparency in drop-filter cavity-waveguide systems, Phys. Rev. Lett. 96 (153601)

[6] T.D. Ladd, P. van Loock, K. Nemoto, W.J. Munro, Y. Yamamoto, Hybrid quantum repeater based on dispersive CQED interactions between matter qubits and bright coherent light, N. J. Phys. 8 (2006) 184.

[7] K.M. Birnbaum, A. Boca, R. Miller, A.D. Boozer, T.E. Northup, H.J. Kimble, Photon blockade in an optical cavity with one trapped atom, Nature 436 (2005) 87–90.

[8] A. Rauschenbeutel, G. Nogues, S. Osnaghi, P. Bertet, M. Brune, J.M. Raimond, S. Haroche, Coherent operation of a tunable quantum phase gate in cavity QED, Phys. Rev. Lett. 83 (1999) 5166–5169.

[9] G. Nogues, A. Rauschenbeutel, S. Osnaghi, M. Brune, J.M. Raimond, S. Haroche, Seeing a single photon without destroying it, Nature 400 (1999) 239–242.

[10] D.I. Schuster, A.A. Houck, J.A. Schreier, A. Wallraff, J.M. Gambetta, A. Blais, L. Frunzio, J. Majer, B. Johnson, M.H. Devoret, S.M. Girvin, R.J. Schoelkopf, Resolving photon number states in a superconducting circuit, Nature 445 (2007) 515–518.

[11] K. Srinivasan, O. Painter, Linear and nonlinear optical spectroscopy of a strongly coupled microdisk-quantum dot system, Nature 450 (2007) 862–865.

[12] A. Faraon, D. Englund, I. Fushman, N. Stoltz, P. Petroff, J. Vučković, Local quantum dot tuning on photonic crystal chips, Appl. Phys. Lett. 90 (213110).

[13] Y. Akahane, T. Asano, B.-S. Song, S. Noda, High-Q photonic nanocavity in a two-dimensional photonic crystal, Nature 425 (2003) 944–947.

[14] D. Englund, A. Faraon, I. Fushman, N. Stoltz, P. Petroff, J. Vučković, Controlling cavity reflectivity with a single quantum dot, Nature 450 (6) (2007) 857–861.

[15] H. Altug, J. Vuckovic, Polarization control and sensing with two-dimensional coupled photonic crystal microcavity arrays, Opt. Lett. 30 (9) (2005) 982–984.

[16] T. Yoshie, A. Scherer, J. Hendrickson, G. Khitrova, H.M. Gibbs, G. Rupper, C. Ell, O.B. Shchekin, D.G. Deppe, Vacuum Rabi splitting with a single quantum dot in a photonic crystal nanocavity, Nature 432 (2004) 200–203.

[17] K. Hennessy, A. Badolato, M. Winger, D. Gerace, M. Atature, S. Gulde, S. Falt, E.L. Hu, A. Imamoglu, Quantum nature of a strongly coupled single quantum dot-cavity system, Nature 445 (2007) 896–899.

[18] E. Peter, P. Senellart, D. Martrou, A. Lemaître, J. Hours, J.M. Gérard, J. Bloch, Exciton-photon strong-coupling regime for a single quantum dot embedded in a microcavity, Phys. Rev. Lett. 95 (6) (2005) 067401, http://link.aps.org/abstract/PRL/v95/e067401.

[19] J.P. Reithmaier, G. Sek, A. Loffler, C. Hofmann, S. Kuhn, S. Reitzenstein, L.V. Keldysh, V.D. Kulakovskii, T.L. Reinecke, A. Forchel, Strong coupling in a single quantum dotsemiconductor microcavity system, Nature 432 (2004) 197–200.

[20] C. Santori, D. Fattal, J. Vučković, G.S. Solomon, E. Waks, Y. Yamamoto, Submicrosecond correlations in photoluminescence from inas quantum dots, Phys. Rev. B 69 (20) (2004) 205324.

[21] S.M. Tan, A computational toolbox for quantum and atomic physics, J. Opt. B: Quant. Semiclass. Opt. 1 (1999) 424–432.

[22] D.P. DiVincenzo, The physical implementation of quantum computation, Fortschr. Phys. 48 (2000) 771–783.

[23] Q. Turchette, C. Hood, W. Lange, H. Mabuchi, H.J. Kimble, Measurement of conditional phase shifts for quantum logic, Phys. Rev. Lett. 75 (1995) 4710–4713.

[24] N. Imoto, H. Haus, Y. Yamamoto, Quantum nondemolition measurement of the photon number via the optical Kerr effect, Phys. Rev. A 32 (1985) 2287–2292.

[25] I. Fushman, D. Englund, A. Faraon, N. Stoltz, P. Petroff, J. Vuckovic, Controlled phase shifts with a single quantum dot, Science 320 (5877) (2008) 769–772, http://www.sciencemag.org/cgi/content/abstract/320/5877/769.

[26] D. Englund, Photonic crystals for quantum and classical information processing, Ph.D. thesis, Stanford University, July 2008.

[27] E. Waks, J. Vuckovic, Dispersive properties and large kerr nonlinearities using dipole-induced transparency in a single-sided cavity, Phys. Rev. A (Atomic Mol. Opt. Phy.) 73 (4) (2006) 041803, http://link.aps.org/abstract/PRA/v73/e041803.

[28] I.L. Chuang, Y. Yamamoto, Simple quantum computer, Phys. Rev. A 52 (5) (1995) 3489–3496.

[29] K. Nemoto, W.J. Munro, Nearly deterministic linear optical controlled-not gate, Phys. Rev. Lett. 93 (25) (2004) 250502.

[30] M.A. Nielsen, I.L. Chuang, Quantum Computation and Quantum Information, Cambridge University Press, Cambridge, 2000.

[31] D. Englund, A. Faraon, B. Zhang, Y. Yamamoto, J. Vuckovic, Generation and transfer of single photons on a photonic crystal chip, Opt. Express 15 (2007) 5550–5558.

[32] D. Englund, D. Fattal, E. Waks, G. Solomon, B. Zhang, T. Nakaoka, Y. Arakawa, Y. Yamamoto, J. Vučković, Controlling the spontaneous emission rate of single quantum dots in a two-dimensional photonic crystal, Phys. Rev. Lett. 95 (2005) 013904.

[33] A. Faraon, I. Fushman, D. Englund, N. Stoltz, P. Petroff, J. Vuckovic, Coherent generation of nonclassical light on a chip via photon-induced tunneling and blockade, quant-ph/0804.2740v1.